



Investigation of Structural, Electronic, Optic and Elastic Properties of Perovskite RbGeCl₃ Crystal: A First Principles Study

Fatma ERDINC¹ , Emel KILIT DOGAN^{1,*} , Harun AKKUS¹ 

¹Van Yüzüncü Yıl University, Department of Physics, 65080, Van, Turkey

Highlights

- Structural, electronic, optic, elastic properties are investigated for perovskite RbGeCl₃ crystal.
- Density Functional Theory (DFT) is used for the investigation of those properties.
- Study performed within the generalized gradient approximation and the local density approximation.
- The calculated electronic band structure shows that the RbGeCl₃ has a direct band gap.
- This compound is a semiconducting material with a wide bandgap.

Article Info

Received: 26/07/2018

Accepted: 18/03/2019

Keywords

Density functional theory

RbGeCl₃

Electronic properties

Optic properties

Abstract

Some physical properties of RbGeCl₃ crystal are investigated with ABINIT computer program within the generalized gradient approximation (GGA) and the local density approximation (LDA), using density functional theory (DFT). We studied the geometry optimization, electronic band structure, electron density of states, optical properties such as the dielectric functions, reflectivity, refractive index, extinction coefficients, energy-loss functions for volume, the effective number of valence electrons per unit cell and elastic properties of RbGeCl₃. The calculated electronic band structure shows that the RbGeCl₃ has a direct band gap and this compound is a semiconducting material with a wide bandgap.

1. INTRODUCTION

The production and storage of energy are the probably two important concerns of all times. In this century new materials that can be used for energy production and storage are exploring by the scientists. By virtue of its availability and low environmental outcome, solar energy is one of the most important inexhaustable energy source [1]. By the investigation on the physical structures and properties of the materials, it is seen that perovskites, especially halide perovskites have a high photovoltaic performance [2] which is important for solar cells.

Perovskites was discovered by Gustav Rose in 1839 and its structure was described by Lev. A. Perovski and still attracts attentions of scientists on a very large spectrum of investigation areas. The class of perovskites adopt the chemical formula as ABX₃, where A is a monovalent cation (e.g., Cs⁺, Rb⁺ ...), B is a bivalent metal cation (e.g., Pb²⁺, Sn²⁺ or Ge²⁺) and X is a halide anion (e.g Cl⁻, Br⁻, I⁻). When X=O (oxygen) then it is called oxide perovskites, when X= inorganic halide (I, Cl, Br) it is called halide perovskites and the other subgroup is hybrid organic-inorganic halide perovskite, generally denoted as CH₃NH₃PbI₃ (MAPbI₃) [3, 4].

Oxide, iodide and hybrid perovskites have been studied in detail [5]. Most of the properties of chloride perovskites are waiting to be revealed.

*Corresponding author, e-mail: ekilit@yyu.edu.tr

Halide perovskites are semiconductors with a direct band gap. They have high light absorption coefficients, high carrier mobility, adjustable spectral absorption ranges and band gap, long charge diffusion lengths, intense photoluminescence, low rates of non-radiative charge recombination superior charge transfer properties [1, 6-8].

These admirable properties have drawn an attention on halide perovskites. By these properties halide perovskites have a large application areas on developing high performance optoelectronic devices such as photodetectors, solar cells, transistors, light-emitting diodes and lasers etc. [3,4,7,9]. Usually, halide perovskites are simply processed into polycrystalline thin films on various substrates for optoelectronic applications. These devices are also cheap and easy to be fabricated [4]. On the other hand some studies in the literature on halide perovskites are focused on the effect of the material composition and morphology on to these properties, and effect of these properties on device performance [10].

A group of halide perovskites with A =Rb, Cs, B = Cd, Ge, and X = Cl, Br, I are revealed as a new group of nonlinear optical materials, which have a wide NLO applications from visible to infrared region such as difference-frequency mixing, optical parametric generation and amplification.

The second-order nonlinear optical (NLO) materials are very important in the field of optics such as laser frequency transformation and optical oscillation/enhancement [11, 12]. Various crystals used in ultraviolet and visible regions, for inorganic second-order NLO materials. But in the infrared region the current materials, are inadequate for applications. So the explorations for new materials in infrared region becomes an important problem for NLO research area [11, 13]. Also some scientists are focused on the halide perovskite nanowires for second-order nonlinear optics [14].

Since there are a few studies about RbGeCl₃ we preferred this crystal among halides. One of them is performed by Messer, he prepared RbGeCl₃ from RbCl and Ge(II) in 6 N HCl or by reaction of RbCl with HGeCl₃, determined the crystal structure and discussed the anionic framework of RbGeCl₃ [15]. The other work carried out by Tang and his coworkers, they synthesized the hydrated rubidium Germanium chloride (RbGeCl₃.x(H₂O)) and identified the non-linear optical properties of hydrated rubidium germanium chlorate [11].

Since RbGeCl₃ has an important role on halide perovskites in regard of non-linear optical materials and since there is no studies in the literature in detail, we performed a further study on this crystal. RbGeCl₃ crystal has two phases, monoclinic and orthorhombic phases. In this study we investigated the structural, electronic, optical and elastic properties of monoclinic RbGeCl₃ crystal using Density Functional Theory (DFT) within the Generalized Gradient Approximation (GGA) and the Local Density Approximation (LDA).

2. COMPUTATIONAL DETAILS

In order to investigate the structural, electronic, optical and elastic properties of RbGeCl₃ halide perovskite we have used the ABINIT [16] (version 7.10.1) code within the GGA and the LDA. For the norm conserving pseudopotentials the self-consistent FHI (Fritz Haber Institute)-type [17] with the Troullier-Martins scheme [18] have been used. The conjugate gradient minimization method [19] was used to solve the Kohn-Sham equations [20]. In order to take into account the exchange-correlation effects, we used the Perdew-Burke-Ernzerhof (1996) [21] generalized gradient and Ceperley-Alder Perdew-Wang local density functional pseudopotentials (1992) [22]. For the electronic wave functions, the plane waves were used as the basis set. For Rb atoms 1 electron with the 5s¹ electronic configuration, for Ge atoms 4 electrons with the 4s² and 4p² electronic configuration, and for Cl atoms 7 electrons with the 3s² and 3p⁵ electronic configuration were taken as the true valence electrons. After the optimization we obtained the cutoff energy as 30 Hartree and Monkhorst-Pack mesh grid [23] as 10x10x10 with 250 k-points.

3. RESULTS

3.1. Structural Properties

The perovskite RbGeCl_3 crystal is in monoclinic structure, and its space group is $P2_1/m$ with space group number 11. RbGeCl_3 has 10 atoms per unit cell. The atomic positions of these atoms are given in Table 1. First of all, we performed geometry optimization after cut-off energy and k-points optimizations, in order to analyze the structural properties of RbGeCl_3 . We took the lattice parameters from the literature [15], and used them in geometry optimization, we plotted total energy vs. volume graphs for the GGA (Figure 1a) and for the LDA (Figure 1b). The minimum points of total energy corresponds to the stable point of the crystal. At this stable point, volume of RbGeCl_3 was calculated as 2058.996 Bohr^3 for GGA and 1791.434 Bohr^3 for LDA. For this stable statement, we calculated the lattice parameters of monoclinic RbGeCl_3 crystal for the GGA and the LDA. We also compared our results with the lattice parameters data that we found from the literature [24] (Table 2). As can be seen from Table 2, GGA gives a lattice parameter which is closer to the experimental one than the LDA. But we wanted to use both the GGA and the LDA in our all calculations in order to demonstrate the difference between them for RbGeCl_3 perovskite crystal. After the geometry optimization, we got the pressure values corresponds to each volume values, and we plotted the graph of Pressure vs. Volume for the GGA (Figure 1c) and for the LDA (Figure 1d). From the graphs one can see that the volume values are decreasing while and the pressure values are increasing, as expected. Also, one can check that the volume value of the stable statement corresponds to the zero (0 GPa) pressure value for both the GGA and the LDA.

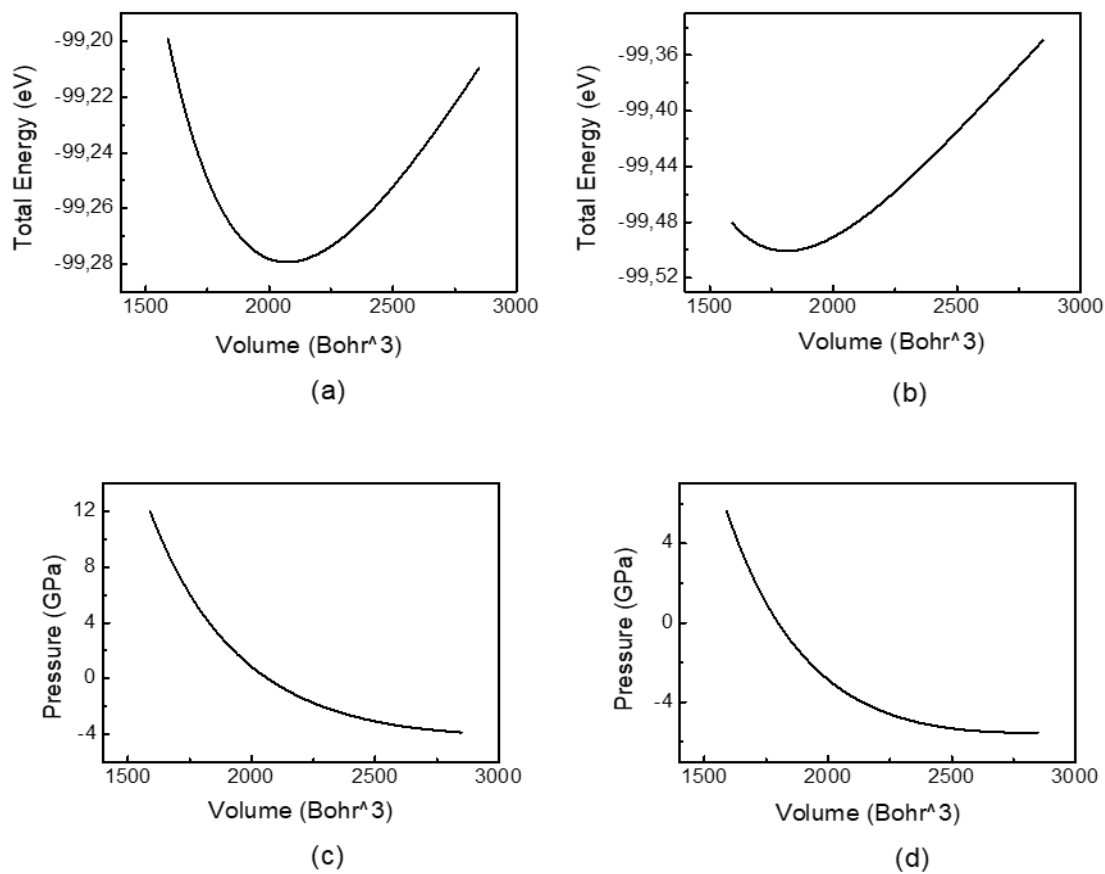


Figure 1. Total energy with respect to volume; a) for GGA b) for LDA. Pressure- volume behaviour of RbGeCl_3 ; c) for GGA and d) for LDA

Table 1. The atomic positions in the unit cell of RbGeCl_3 crystal [15]

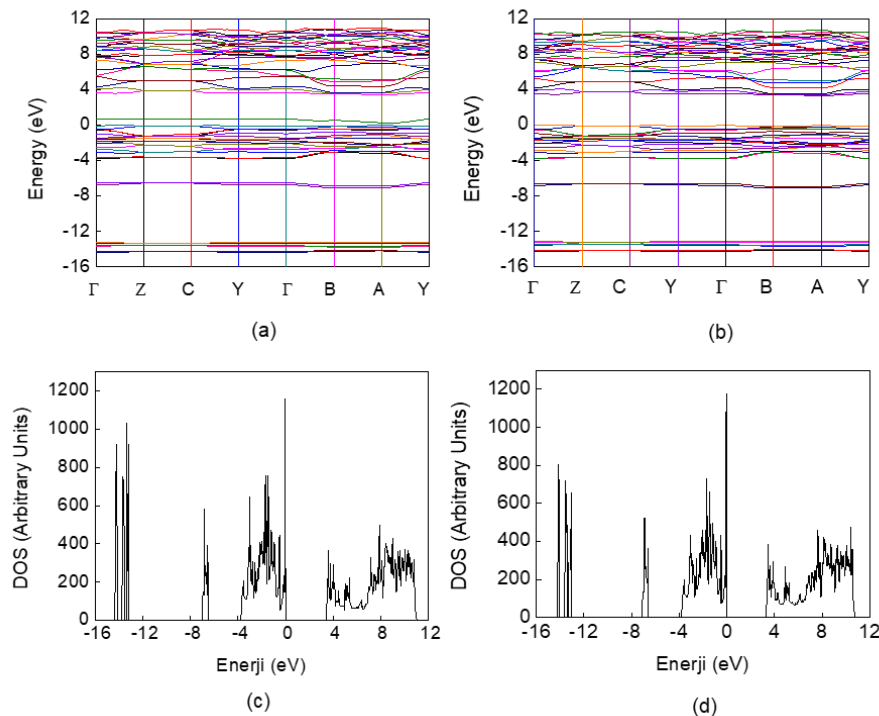
	Site	x	y	z
Rb	2e	0.2943	0.7500	0.6743
Ge	2e	0.1205	0.2500	0.0738
Cl	4f	0.3233	0.0062	0.1878
Cl	2e	0.1256	0.2500	0.6761

Table 2. The experimental [15] and the calculated (present work) values of lattice parameter of monoclinic RbGeCl_3 crystal

Lattice parameters (Bohr)	Experimental values [15]	Calculated (GGA) (Present work) Minimum Energy: -99.28 eV	Calculated (LDA) (Present work) Minimum Energy: -99.50 eV	Ref. [24]
a	15.0951	14.8851	13.8351	15.7999
b	13.1166	12.9066	11.8566	13.5983
c	10.9604	10.7504	9.7004	11.1757

3.2. Electronic Properties

To be able to investigate the electronic properties of RbGeCl_3 perovskite we used pseudopotential method based on density functional theory within both the generalized gradient and the local density approximations. The calculated band structure of RbGeCl_3 for the GGA is given in Figure 2a and for the LDA is given in Figure 2b, where the Fermi energy level was set to origin for both graphs. This crystal has 26 valence bands, additionally we demonstrated 26 conducting bands. One can see from Figures 2a and 2b that RbGeCl_3 has a direct band gap with the value of 3.27 eV for GGA and 3.28 eV for LDA both occur at A high symmetry point in the Brillouin Zone. From these graphs we can classify RbGeCl_3 as a semiconductor with a wide band gap.

**Figure 2.** Electronic band structure; a) for GGA b) for LDA. Density of states graphs; c) for GGA and d) for LDA

We also investigated the density of states (DOS) then calculated and plotted the total density of states of RbGeCl_3 under both the GGA (Figure 2c) and the LDA (Figure 2d). From these figures, one can see that, the contribution of valence electrons to the DOS is between -16.57 eV and -2.60 eV for GGA and between -16.36 eV and -2.18 eV for LDA. Conducting electrons contribute to DOS above 0.73 eV for GGA and above 0.91 eV for LDA. The partial density of states according to Rb (Figure 3a), Ge (Figure 3b) and Cl (Figure 3c) atoms are given in Figure 3. It can be noticed that Rb atoms contribute to conduction bands, Ge atom contribute to valence bands and Cl atoms contribute to deep valence bands mostly, as can be seen from partial density of states graphs.

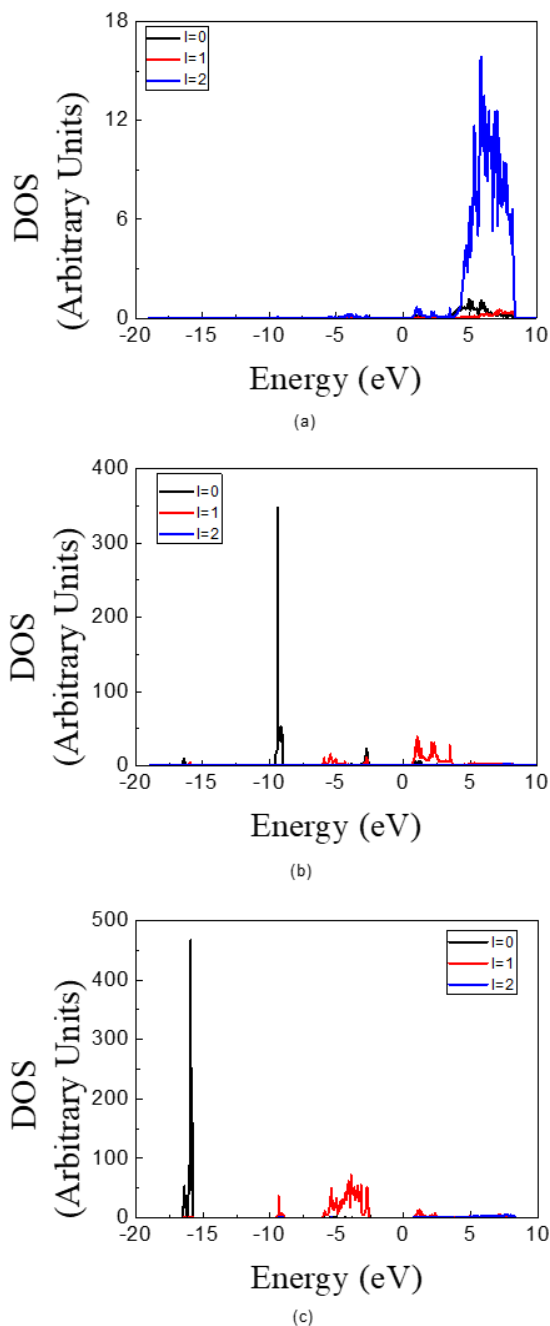


Figure 3. The partial density of a) Rb, b) Ge and c) Cl atoms in RbGeCl_3 crystal

3.3. Optical Properties

In this part, we investigated the optical response and properties of RbGeCl_3 . First of all, we calculated the real (ϵ_1) and imaginary (ϵ_2) parts of complex dielectric function. The real part, which shows the physical properties of a crystal, was plotted for RbGeCl_3 in Figure 4a under the GGA and in Figure 4b under the LDA. The imaginary part corresponds to the energy loss of photons in a material and electron transition between electronic bands, plotted in Figure 4c for the GGA and in Figure 4d for the LDA, respectively. In all these graphs, the variation of optical properties against photon energies towards a- b- and c- crystal axis were given. Since RbGeCl_3 crystal is in monoclinic structure, the physical properties of this crystal depends on the direction.

In real dielectric function (ϵ_1) graphs (Figures 4a and 4b) the regions which decreases with the increasing of the photon energy gives the anomalous dispersion region. When ϵ_1 values take zero values at some photon energies, these points gives us plasmon frequencies. Also when ϵ_1 values becomes negative in some regions which means that there is a reflection of the incident electromagnetic waves. Those points that corresponds to plasmon frequencies and the negative regions of ϵ_1 can be examined from Figures 4a and 4b. The static dielectric constants, $\epsilon_1(0)$, were calculated as 3.205 towards a, 3.527 towards b and 3.821 towards c-directions for the GGA and 3.797 towards a, 4.141 towards b and 4.791 towards c-directions for the LDA.

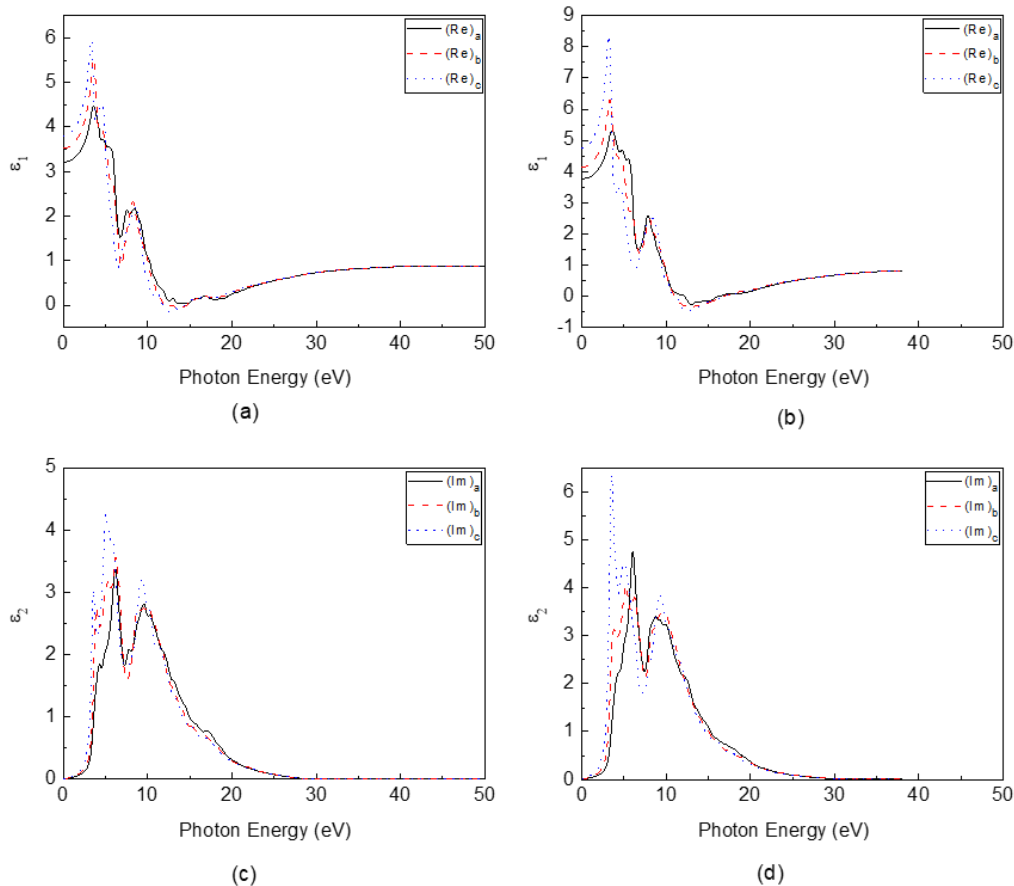


Figure 4. The real part of the complex dielectric function a) for GGA b) for LDA. The imaginary part of the complex dielectric function c) for GGA d) for LDA

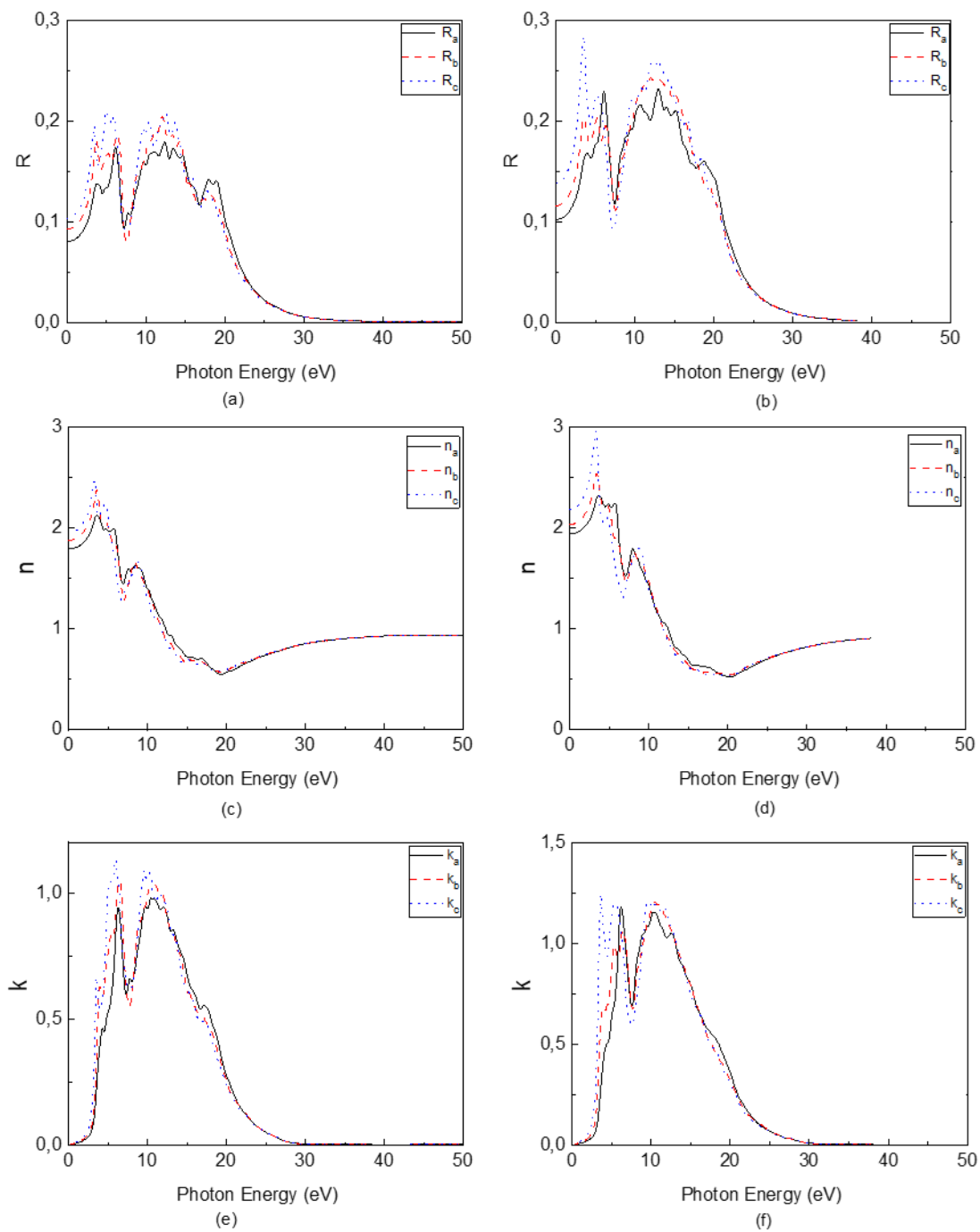


Figure 5. Reflectivity a)for GGA b)for LDA, refractive index c)for GGA d)for LDA, extinction coefficients e)for GGA f)for LDA of $RbGECI_3$ crystal

The peaks in ε_2 shows the transitions of electron from valence to conduction bands. The first value that the transition starts was noticed approximately as 3.27 eV for the GGA and 3.28 eV for the LDA.

The characteristics of reflectivity was calculated and plotted in Figure 5a (GGA) and Figure 5b (LDA). The static refractive index $n(0)$ was obtained as 1.95 for a, 1.89 for b and 1.79 for c directions in the GGA (Figure 5c) 2.19 for a, 2.04 for b and 1.94 for c directions in the LDA (Figure 5d). The local minimum of extinction coefficient k shown in Figure 5e for the GGA and 5f for the LDA, corresponds to the zero of ε_1 . Loss function refers to the energy loss of a fast electron crossing over the crystal. The peak values are related with the plasmon resonance. The frequency of the overall oscillation of valence electrons in a crystal is called plasmon frequency. Figures 5g and 5h show the loss function behaviour against photon energy for

the GGA and the LDA, respectively. The effective number of electrons that can be found in the unit cell of a crystal, N_{eff} , specifies the contribution which is done to optical functions during the transition between the electronic bands. Effective number of valence electrons are calculated and plotted with respect to the photon energy with the GGA in Figure 5i and with the LDA in Figure 5j. N_{eff} values first increases then stays stable. After that point there is no any transitions between electronic bands.

3.4. Elastic Properties

First we calculated the elastic constants of RbGeCl₃ crystal by means of density functional theory within the local density approximation. There would be 36 elastic constants, it decreased to 21 because of the symmetry, then since Laue group of RbGeCl₃ is 2/m, the number of independent elastic constant decreased to 13, as shown below.

Table 3. Values of the elastic constants of RbGeCl₃ crystal

C_{ij}	Calculated value (GPa)
C_{11}	26.73
C_{12}	21.62
C_{13}	23.91
C_{15}	-4.24
C_{22}	41.86
C_{23}	29.53
C_{25}	1.43
C_{33}	64.64
C_{35}	-0.58
C_{44}	4.41
C_{46}	0.80
C_{55}	2.90
C_{66}	2.07

It can be seen from Table 3 that we have found negative elastic coefficients of RbGeCl₃ crystal. The diagonal elements of the elastic coefficients (C_{11} , C_{22} , C_{33} ...) which are called principle components are all positive for our crystal. The negative components are belong to off-diagonal components which are called shear components. Stability of the crystal requires the matrix of elastic constants ($C_{\mu\nu}$, $\mu, \nu = 1, 2, \dots, 6$) to be positive definite. A necessary and sufficient condition for this case is that the 6 principal components of this matrix must be positive. The off-diagonal elements may have either signs, positive or negative [25]. So our calculated elastic constants confirm to stability rules. But how can an elastic constant be negative How can this phenomenon be explained? According to our searches and knowledge a material can show negative elastic coefficients, for example post-buckled elements which already have some stored energy. It is possible to give a definition as; if the deformation is opposite to the force direction then negative elastic coefficient occurs, like auxetic bodies. Auxetic bodies are the materials which contain the property of counter-intuitively expanding when being stretched [26]. In positive elastic coefficient case they are in same directions. Also there is another definition which is as follows: when one of the constituent element of a material has immensely high stiffness than the others, this material can have a negative elastic coefficient. Mostly it is seen in composite materials. When we look at our crystal, we see that the stiffness of Germanium is 91,9 GPa [27] which is immensely bigger than Rubidium (2,4 GPa) [28] and Chloride (no stiffness) [29].

$$C_{ij} = \begin{bmatrix} C_{11} & C_{12} & C_{13} & 0 & C_{15} & 0 \\ \cdot & C_{22} & C_{23} & 0 & C_{25} & 0 \\ \cdot & \cdot & C_{33} & 0 & C_{35} & 0 \\ 0 & 0 & 0 & C_{44} & 0 & C_{46} \\ \cdot & \cdot & \cdot & 0 & C_{55} & 0 \\ 0 & 0 & 0 & \cdot & 0 & C_{66} \end{bmatrix} \quad (1)$$

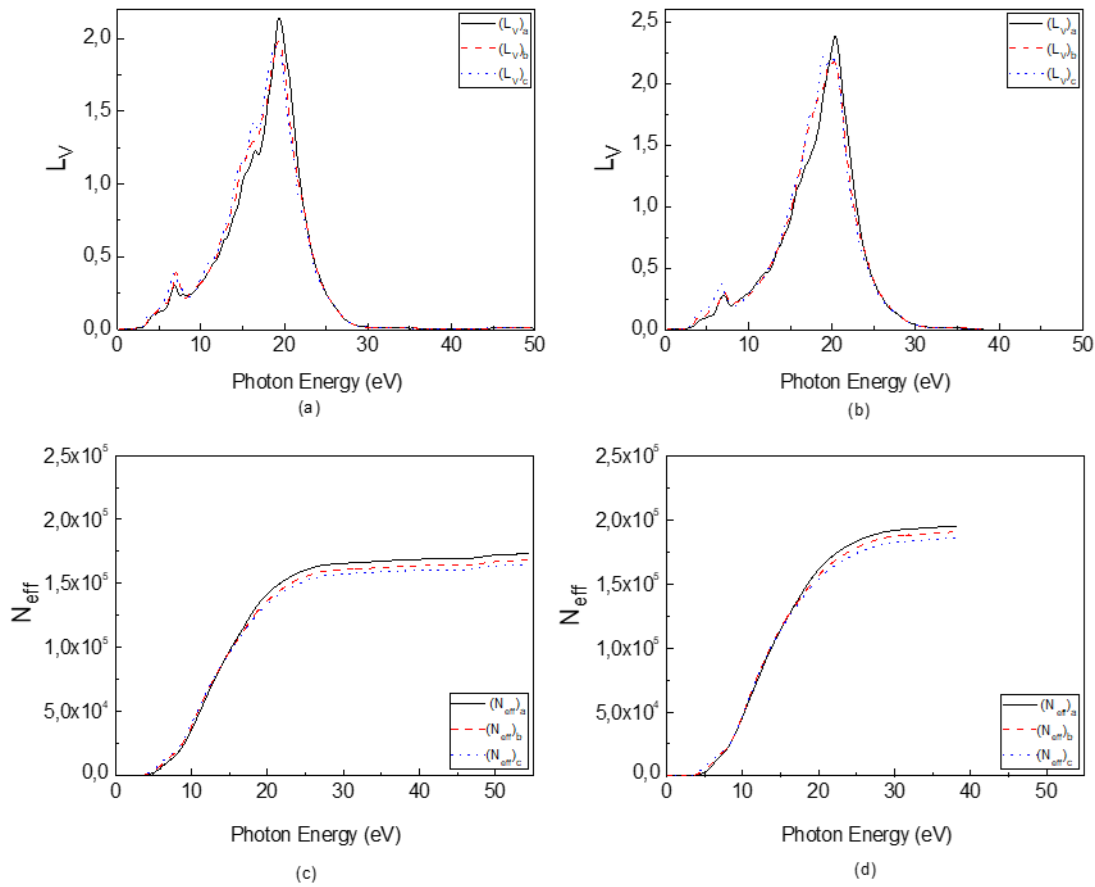


Figure 6. Energy-loss functions for volume g)for GGA h) for LDA, the effective number of valence electrons per unit cell i)for GGA j) for LDA of $RbGeCl_3$ crystal

The ratio between bulk modulus and shear modulus is a kind of measurement of elasticity or fragility of a material. The critical ratio equals to 1.75. The smaller values show fragile property. We found this ratio as 6.27, so our material has a elasticity property. Elasticity properties can be also understood by comparing the poisson ratios. Critical value is 1/3, smaller values than this critical value shows that materials fragile property.

There are also other critical modules that figures out the elastic structure of a material. We calculated Voight Bulk Modulus, Hill Bulk Modulus, Voight Shear modulus etc. as can be seen from Table 4.

Table 4. Some elastical properties of $RbGeCl_3$ crystal

Property	Symbol	Calculated value
Voight Bulk Modulus	B_V	31.48 (GPa)
Reuss Bulk Modulus	B_R	19.74 (GPa)
Hill Bulk Modulus	B_H	25.61 (GPa)
Voight Shear Modulus	G_V	5.75 (GPa)
Reuss Shear Modulus	G_R	2.41(GPa)
Hill Shear Modulus	G_H	4.08 (GPa)
Young Modulus	E	11.63 (GPa)
Poisson Ratio	ν	0.42
Lame Constant-1	μ	4.08 (GPa)
Lame Constant-2	λ	22.89 (GPa)
Elasticity (Pugh) Coefficient	K	6.28

4. CONCLUSIONS

In present work, we studied the geometry optimization, electronic band structure, electron density of states, optical properties such as the photon energy dependent dielectric functions, reflectivity, refractive index, extinction coefficients, energy-loss functions for volume, the effective number of valence electrons per unit cell and elastic properties of RbGeCl₃ using ABINIT code within the both GGA and LDA based on the DFT. This crystal has a semiconductor with a wide band gap property with the band gap value 3.27 eV for the GGA and 3.28 eV for the LDA with a direct band gap at high symmetry A point. We have not meet any accessible data except from Materials Project data, for RbGeCl₃ from the literature. Thus, we could not be able to compare our results but, we estimate that this study of us will be a source for further studies about this crystal in the future.

ACKNOWLEDGEMENTS

This work has been supported by The Unit of Scientific Research Projects of Van Yuzuncu Yil University under Project No. 2011-FED-B010.

CONFLICTS OF INTEREST

No conflict of interest was declared by the authors.

REFERENCES

- [1] Zhang, W., Eperon, G. E. and Snaith, H. J. "Metal halide perovskites for energy applications", *Nature Energy*, 1: 16048-8, (2016).
- [2] Stoumpos, C. C. and Kanatzidis, M. G. "Halide Perovskites: Poor Man's High- Performance Semiconductors", *Advanced Materials*, 28: 5778-5793, (2016).
- [3] Chen, Q., De Marco, N., Yang, Y., Song, T. B., Chen, C. C., Zhao, H., Hong, Z., Zhou, H. and Yang, Y. "Under the spotlight: The organic-inorganic hybrid halide perovskite for optoelectronic applications", *Nano Today*, 10: 355-396, (2015).
- [4] Chen, S. and Shi, G. "Two- Dimensional Materials for Halide Perovskite- Based Optoelectronic Devices" *Advanced Materials*, 29: 1605448-31, (2017).
- [5] McMurdie, H. F., de Groot, J., Morris, M. and Swanson, H. E. "Crystallography and preparation of some ABCl₃ compounds", *Journal of Research of the National Bureau of Standards-A. Physics and Chemistry*, 73A: 621-626, (1969).
- [6] Kumawat, N. K., Tripathi, M. N., Waghmare, U. and Kabra, D. "Structural, optical, and electronic properties of wide bandgap perovskites: experimental and theoretical Investigations", *The Journal of Physical Chemistry*, 120: 3917-3923, (2016).
- [7] Zhao, Y. and Zhu, K. "Organic-inorganic hybrid lead halide perovskites for optoelectronic and electronic applications", *Chemical Society Reviews*, 45: 655-689, (2016).
- [8] Roghabadi, F. A., Ahmadi, V. and Aghmiani, K. O. "Organic-Inorganic Halide Perovskite Formation: In Situ Dissociation of Cation Halide and Metal Halide Complexes during Crystal Formation", *Journal of Physical Chemistry C*, 121: 13532-13538, (2017).
- [9] Veldhuis, S. A., Boix, P. P., Yantara, N., Li, M., Sum, T. C., Mathews, N. and Mhaisalkar, S. G. "Perovskite materials for light- emitting diodes and lasers", *Advanced Materials*, 28: 6804-6834, (2016).

- [10] Adinolfi, V., Peng, W., Walters, G., Bakr, O. M. and Sargent, E. H. "The Electrical and Optical Properties of Organometal Halide Perovskites Relevant to Optoelectronic Performance", *Advanced Materials*, 30: 1700764-13, (2018).
- [11] Tang, L. C., Liu, L. Q., Chang, Y. C., Yao, J.H., Huang, J.Y. and Chang, C. S. "Characterization of Nonlinear Optical Properties of Crystal $\text{RbGeCl}_3 \cdot x(\text{H}_2\text{O})$ in Infrared Region", *Japanese Journal of Applied Physics*, 48: 082001-7, (2009).
- [12] Giordmaine, J. A. and Miller, R. C. "Tunable Coherent Parametric Oscillation in LiNbO_3 at Optical Frequencies", *Physical Review Letters*, 14: 973-975, (1965).
- [13] Dmitriev, V. G., Gurzadyan, G. G. and Nikogosyan, D. N., *Handbook of Nonlinear Optical Crystals*, Springer Press, Berlin. p. 100, (1999).
- [14] Yuan, C., Li, X., Semin, S., Feng, Y., Rasing, T. and Xu J. "Chiral Lead Halide Perovskite Nanowires for Second-Order Nonlinear Optics", *Nano Letters*, 18: 5411-5417, (2018).
- [15] Messer, D., "Die Kristallstruktur von RbGeCl_3 /The Crystal Structure of RbGeCl_3 ", *Zeitschrift für Naturforschung B*, 33b: 366-369, (1978).
- [16] Gonze, X., Beuken, J. M., Caracas, R., Detraux, F., Fuchs, M., Rignanese, G.M., Sindie, L., Verstrate, M., Zerah, G., Jollet, F., Torrent, M., Roy, A., Mikami, M., Ghosez, P., Raty, J. Y. and Allan, D. C. "First-principles computation of material properties: the ABINIT software Project", *Computational Materials Science*, 25: 478-492, (2002).
- [17] Fuchs, M. and Scheffler, M. "Ab initio pseudopotentials for electronic structure calculations of polyatomic systems using density-functional theory", *Computer Physics Communications*, 119: 67-98, (1999).
- [18] Troullier, N. and Martins, J. L. "Efficient pseudopotentials for plane-wave calculations", *Physical Review B*, 43: 1993-2006, (1991).
- [19] Payne, M.C., Teter, M. P., Allan, D. C., Arias, T. A. and Joannopoulos, J. D. "Iterative minimization techniques for ab initio total-energy calculations: molecular dynamics and conjugate gradients", *Reviews of Modern Physics*, 64: 1045-1098, (1992).
- [20] Khon, W. and Sham, L. J. "Self-Consistent Equations Including Exchange and Correlation Effects", *Physical Review*, 140:A1133-A1138, (1965).
- [21] Perdew, J. P., Chevary, J. A., Vosko, S. H., Jackson, K. A., Pederson, M. R., Singh, D. J. and Fiolhais, C. "Atoms, molecules, solids, and surfaces: Applications of the generalized gradient approximation for exchange and correlation", *Physical Review B*, 46: 6671-6687, (1992).
- [22] Perdew, J. P., Burke, K. and Ernzerhof, M. "Generalized Gradient Approximation Made Simple", *Physical Review Letters*, 77: 3865-3868, (1996).
- [23] Monkhorst, J.H. and Pack, J.D. "Special points for Brillouin-zone integrations", *Physical Review B*, 13: 5188-5192, (1976).
- [24] Internet: Materials Project. <https://materialsproject.org/materials/mp-27369>, (2018).
- [25] Horn, R. A., and Johnson, C. R., *Matrix Analysis*, Cambridge University Press, Cambridge. p. 40 and 404, (1990).

- [26] Teodorescu, P. P., *Treatise on Classical Elasticity, Theory and Related Problems*, Springer Press, Berlin. p. 29,(2010).
- [27] Maksud, M., Yoo, J., Harris, C. T., Palapati, N. K. R. and Subramanian, A., “Young’s modulus of [111] germanium nanowires”, *APL Materials*, 3: 116101, (2015).
- [28] Internet: Technical data for Rubidium. <http://periodictable.com/Elements/037/data.html> , (2019).
- [29] Internet: Technical data for Chlorine. <http://periodictable.com/Elements/017/data.html> , (2019).